Published in final edited form as:
Behav Brain Res. 2011 January 1; 216(1): 332–340. doi:10.1016/j.bbr.2010.08.013.

FOCAL EXPRESSION OF MUTATED TAU IN ENTORHINAL CORTEX NEURONS OF RATS IMPAIRS SPATIAL WORKING MEMORY

Julio J. Ramirez[a,b,*], **Winona E. Poulton**[b], **Erik Knelson**[b], **Cole Barton**[a], **Michael A. King**[c,d], and **Ronald L. Klein**[e]

[a]Department of Psychology, Davidson College, Davidson, NC 28035

[b]Neuroscience Program, Davidson College, Davidson, NC 28035

[c]Department of Pharmacology and Therapeutics, University of Florida College of Medicine, Gainesville, FL 32610

[d]NF/SG Veterans Administration Medical Center, Gainesville, FL 32608

[e]Department of Pharmacology, Toxicology and Neuroscience, LSUHSC, Shreveport, LA 71130

Abstract

Entorhinal cortex neuropathology begins very early in Alzheimer's disease (AD), a disorder characterized by severe memory disruption. Indeed, loss of entorhinal volume is predictive of AD and two of the hallmark neuroanatomical markers of AD, amyloid plaques and neurofibrillary tangles (NFTs), are particularly prevalent in the entorhinal area of AD-afflicted brains. Gene transfer techniques were used to create a model neurofibrillary tauopathy by injecting a recombinant adeno-associated viral vector with a mutated human tau gene (P301L) into the entorhinal cortex of adult rats. The objective of the present investigation was to determine whether adult onset, spatially restricted tauopathy could be sufficient to reproduce progressive deficits in mnemonic function. Spatial memory on a Y-maze was tested for approximately three months post-surgery. Upon completion of behavioral testing the brains were assessed for expression of human tau and evidence of tauopathy. Rats injected with the tau vector became persistently impaired on the task after about six weeks of postoperative testing, whereas the control rats injected with a green fluorescent protein vector performed at criterion levels during that period. Histological analysis confirmed the presence of hyperphosphorylated tau and NFTs in the entorhinal cortex and neighboring retrohippocampal areas as well as limited synaptic degeneration of the perforant path. Thus, highly restricted vector-induced tauopathy in retrohippocampal areas is sufficient for producing progressive impairment in mnemonic ability in rats, successfully mimicking a key aspect of tauopathies such as AD.

[*]Address correspondence to: Julio J. Ramirez, Ph.D. Department of Psychology and Neuroscience Program Box 7017 Watson Building, Room 202 Davidson College, Davidson, North Carolina 28035 U.S.A. TEL: (704) 894-2888 FAX: (704) 894-2512 juramirez@davidson.edu.

Keywords

Alzheimer's disease; hippocampal formation; learned alternation; P301L; retrohippocampal area; tauopathy; Y-maze

1. INTRODUCTION

Tau protein pathology underlies a wide variety of neurological disorders, including argyrophylic grain disease, Pick's disease, progressive supranuclear palsy, frontotemporal dementia and parkinsonism linked to chromosome 17 (FTDP-17; reviewed in Tolnay and Probst, 1999, 2002). The most prevalent and costly tauopathy is Alzheimer's disease (AD), in which neurofibrillary tangle pathology is mixed with amyloid plaques. Of these two hallmark features of AD, the amyloid-laden neuritic plaques and metabolites of the amyloid precursor protein (APP) have received extensive scientific attention as causal determinants of dementia and neuropathology (reviewed in Carter and Lippa, 2001; Sinha and Lieberburg, 1999; Wasling et al., 2009). It has been increasingly recognized, however, that neurofibrillary tangle (NFT) pathology contributes to the behavioral consequences of AD (Brunden et al., 2008). NFTs are composed of abnormally-hyperphosphorylated aggregations of the microtubule-associated protein tau, which under normal conditions is essential to proper microtubule functioning critical for neurons that must maintain specialized compartments far from the nucleus for many years (Buée et al., 2000).

Since Hyman et al.'s reports (1984; 1986) that AD-induced loss of the parahippocampal region may isolate the hippocampal formation from its efferent and afferent connections resulting in cognitive decline, the parahippocampal region, especially the entorhinal cortex (EC), has come under scrutiny as a possible early target of AD. In their assessment of postmortem human brains from nondemented and demented individuals, Braak and Braak (1991) observed that a signature trait for AD brains was the progression of NFT and neuropil threads from the transentorhinal layer Pre-α in the earliest stages (stages I–II) to the final widespread destruction of isocortical association areas (stages V–VI). Several investigations (Garcia-Sierra et al., 2000; Giannakopoulos et al., 2003; Mitchell et al., 2002; Thal et al., 2000) have since confirmed that the tau pathology of the parahippocampal area and the perforant path, the entorhinal efferent to the hippocampal formation, as well as its target zone in the hippocampus are significantly related to the cognitive decline evident in Alzheimer's patients.

Attempting to model the development in the mature brain of a tau-mediated functional disruption between entorhinal neurons and their hippocampal synaptic targets, we selectively expressed a human tauopathy-causing mutant gene (P301L) in the adult rat EC. Despite the fact that tau mutations are not observed in AD, mutations that cause other tauopathies stimulate comparable biochemical and cytological neurofibrillary pathology and have been widely used to introduce tauopathy into AD models with amyloid pathology. The P301L mutation that causes an inherited FTDP-17 has been instrumental for exploring behavioral and neural manifestations of disease common to both inherited and sporadic tauopathies (Ramsden et al., 2005; Santacruz et al., 2005; Spires et al., 2006).

Although transgenic mouse models are powerful approaches to understanding how such mutations might impair neural functioning, a common outcome of mutant tau transgenic mice has been brain regional patterns of tau pathology that differ from the human diseases. Atypical behavioral sequelae such as early motor impairment (reviewed in Eriksen and Janus, 2007) associated with these expression patterns further limit the use of such models for unraveling the etiology of progressive dementia. Pathology in widespread regions complicates analysis of behavioral phenomena that may require only specific neuronal populations. Also,

tauopathies generally develop in adults, and expression of mutant tau during brain development and maturation may confound transgenic models. A complementary approach to the transgenic model is somatic cell gene transfer, which allows transduction of mutant genes in specific brain regions at controlled times (Klein et al., 2004). This makes it possible to examine specific disease effects in relative isolation from development as well as the expression of disease-causing genes restricted to the most relevant areas. Here, to test the hypothesis that adult-onset expression of P301L mutated tau in the EC of rats would impair spatial memory functioning in conjunction with tau pathology, we transduced entorhinal neurons by injecting recombinant adeno-associated viral vector serotype 2 (rAAV2) constructed to drive the expression of P301L mutated tau (rAAV2-tau$_{P301L}$), or control rAAV2 constructed to drive the expression of green fluorescent protein (GFP; rAAV2-GFP). The rats were subsequently tested repeatedly for acquisition and retention of a learned spatial alternation task after which their brains were assessed for evidence of tau pathology. The results indicate that targeting the entorhinal area yields a behaviorally and neuropathologically relevant model for AD and other adult-onset tauopathies involving limbic structures and progressive dementia.

2. MATERIALS AND METHODS

2.1 Subjects

Twenty male Sprague-Dawley rats weighing (300–350 g; approximately 90 days of age at the start of the behavioral testing) were purchased from Hilltop Animal Labs Inc. (Scottsdale, PA). Animals were housed individually in cages and maintained on a 12 hour light-dark cycle (lights on at 7:00 am). Animals were food deprived to about 80% of their initial body weight at the beginning of the investigation; they were subsequently allowed to gain five grams each week for the remainder of the testing period. The rats had *ad libitum* access to water. All procedures described here were approved by the Davidson College Institutional Animal Care and Use Committee and were conducted in accordance with the guidelines of the Animal Welfare Act and the National Institutes of Health.

2.2 Apparatus

A gray semi-automated Y-maze was used for all behavioral testing. An approach alley (13 cm high × 13 cm wide × 40 cm long) was separated from two goal arms (13 cm high × 13 cm wide × 47 cm long) by a guillotine door.

2.3 Experimental Design and Behavioral Testing

The rats were randomly assigned to two treatment conditions: 1) bilateral EC injection of rAAV2-tau$_{P301L}$ (Tau, n=10); or 2) bilateral EC injection of rAAV2-GFP (GFP Control, n=10). The behavioral testing procedures were similar to those reported earlier (Ramirez et al., 2007). Briefly stated, before surgery the rats were trained for one week to traverse a maze for food reward (two 45 mg Noyes pellets) according to a random series of forced left and right turns (Gellerman, 1933). Seven days following surgery, the rats were trained to alternate in the Y-maze for two 45 mg Noyes pellets for 11 trials per day (for a total of 10 alternations per training session with 40 sec intertrial intervals). After receiving a reward for the first trial of a session, the rats were reinforced only for correctly alternating their entry into a goal arm on subsequent trials. Testing continued for 12 consecutive weeks (seven days per week for the first two weeks, then five days per week thereafter). The experimenters were blind to the rats' treatment condition. Errors were defined as repeated entry into a previously rewarded goal arm and criterion for acquisition was operationally defined as committing two or fewer errors for three consecutive days (cf. Ramirez and Stein, 1984).

2.4 AAV2 Vector Preparation

We made rAAV2 vectors for either human tau or control GFP transgenes using described methods (Klein et al., 2008). The form of the tau transgene contained the P301L mutation associated with frontotemporal dementia, and four microtubule-binding domains (exons 2−/3−/10+). The expression cassette was flanked with AAV2 terminal repeats for production of recombinant AAV2. The hybrid cytomegalovirus/chicken β-actin promoter and the woodchuck hepatitis post-transcriptional regulatory element were used to drive expression (Klein et al., 2006). Human embryonic kidney 293-T cells were co-transfected with either the tau or the GFP transgene plasmid along with the packaging plasmid needed to make AAV2. The cell lysate was applied to a discontinuous gradient of iodixanol (OptiPrep, Greiner Bio-One, Longwood, FL) and centrifuged. The AAV was then removed, diluted 2-fold with lactated Ringer's solution (Baxter, Deerfield, IL), and then washed and concentrated by Millipore (Billerica, MA) Biomax 100 Ultrafree-15 units. The final stocks were sterilized with Millipore Millex-GV syringe filters into low adhesion tubes (USA Scientific, Ocala, FL). Vectors were aliquoted and stored frozen. Encapsidated genome copies were titered by dot-blot. The titer of the AAV2 tau was 7.2×10^{11} vector genomes (vg)/ml and the rAAV2 GFP was 7.6×10^{11} vg/ml. Equal dose comparisons were made by normalizing titers with the diluent, lactated Ringer's solution.

2.5 Surgical Procedures

Following behavioral training on the Gellerman sequence, the rats sustained surgery under aseptic conditions. After 12 hours of food and water deprivation, the rats were administered an intraperitoneal (ip) injection of 0.1 ml atropine sulfate (0.54 mg/ml) and then anesthetized with an ip injection of sodium pentobarbital (Nembutal, 50 mg/kg). A craniotomy overlying the retrohippocampal area was performed and injections of either the rAAV2-GFP or rAAV2-tau_{P301L} vectors were made into the following stereotaxically defined sites: incisor bar set at −3.4 mm; AP: −8.3, ML: ±3.3, DV: −6.0, and −5.0; and AP: −8.8, ML: ±3.7, DV: −5.0. A 22° beveled tip 10 μL Stoelting Hamilton syringe (51096) was loaded with vector and slowly inserted (10° from vertical [along the medial-lateral axis] for the right hemisphere injections and −10° for the left hemisphere) to the desired depth in one hemisphere and allowed to sit for two minutes prior to injection of the viral vector. Subsequently, viral vector was manually injected at a rate of 0.1 μL/min over the course of 20 minutes for a total of 2.0 μL in each of three injections per hemisphere. Needles were removed after 2 minutes and incisions closed by suture.

2.6 Histological Procedures

After the completion of the 12 week behavioral testing rats were anesthetized deeply with sodium pentobarbital (Nembutal, 100 mg/kg ip) and transcardially perfused with 100 ml 0.1 M sodium chloride chased by 400 ml 4% formaldehyde in 0.1 M phosphate buffered saline pH 7.4 (PBS). After 2 hr at 4° C the brains were extracted into 30% sucrose PBS for cryoprotection and stored refrigerated. The cerebellum was removed and the frontal pole separated by a coronal cut between the septum and hippocampus. The block containing entorhinal cortex and hippocampus was sectioned at −18° C in the horizontal plane using a sliding microtome fitted with a thermoelectric freezing stage. Sections (50 μm) were placed in individual wells of 24-well polypropylene plates (Phenix Research Products, Inc., Candler, NC) containing 400 μl PBS. Sections for immunolabeling were subjected to suppression of endoperoxidative activity by incubation in 400 μl/well 3% hydrogen peroxide in PBS for 5 min, followed by 2 × 5 min 500 μl/well PBS washes. All incubations were conducted on a rotating shaker at room temperature (ca. 21° C). Non-specific binding was blocked by incubation in 2% goat serum in PBS. Primary antibodies (GFP, Molecular Probes A11122, 1:10,000; T14, Zymed 13–1400, 1:1,000; AT8, Pierce Endogen, 1:500; NFT, Chemicon AB1518, 1:200; GFAP, Sigma G3893,

1:400; OX6, Serotec, 1:1,000) diluted in PBS containing 0.1% Triton X-100 detergent plus 0.02% antimicrobial sodium azide, were incubated overnight at 200 μl/well. Following 2 × 15 min 500 μl/well washes, sections were incubated overnight in biotinylated goat anti-rabbit (Dako E0432, 1:1,000) or anti-mouse (Sigma B0529, 1:10,000) secondary antibodies in PBS. After 2 more PBS washes sections were incubated overnight in extravidin-peroxidase (Sigma E2886, 1:1,000), washed twice with 500 μl/well 0.1 M sodium acetate, and reacted 5 min with chromogen solution containing 0.5 mg/ml diaminobenzidine (DAB, Sigma D5637), 0.4 μl/ml 30% hydrogen peroxide. Sections were mounted on chrome-alum subbed slides from 0.1 M saline, dehydrated, and coverslipped with glycerol-gelatin (Sigma GG-1). The Gallyas silver staining method for labeling NFTs was used on a subset of sections (Gallyas, 1971).

Slides were examined on an Olympus BH-2 brightfield and epifluorescence microscope fitted with a Hitachi KP-D581 color digital video camera interfaced with an Integral Tech frame grabber in a desktop computer. Motorized stage and focus (Prior Scientific, Rockland, MA), and image acquisition, were controlled through ImagePro Plus (Media Cybernetics, Silver Springs, MD). Injection tracks were mapped to horizontal sections of the Paxinos and Watson (1986) rat brain atlas.

2.7 AChE Histochemetry

To examine whether P301Ltau expression in entorhinal cortex resulted in deafferentation sufficient to induce dentate cholinergic remodeling, series of coronal frozen sections from brains of rats that received rAAV2-tau$_{P301L}$ or rAAV2-GFP were stained using our microwave acetylcholinesterase (AChE) procedure. A modified Karnovsky-Roots (Karnovsky and Roots, 1964) histochemical reaction for AChE was used to assess whether cholinergic reactive synaptogenesis occurred in response to tauopathy in entorhinal afferent terminal fields (Cotman et al., 1990). Frozen sections were collected individually in 300 μl PBS/well in 24 well untreated culture plates. This was replaced with 250 μl/well 0.1 M sodium acetate pH 6.0 (2 times, 5 min each), then by a preincubation solution for 5–15 min (cupric sulfate, 1.9 mM; potassium ferricyanide, 0.5 mM; sodium citrate, 5.0 mM; ethopropazine, 200uM; 200 μl/well). The culture plate was set directly on crushed ice packed in a Pyrex or polystyrene container, and the 200 μl/well substrate solution (same as preincubation solution plus 0.484 mM acetylthiocholine iodide) was added directly to the preincubation solution. The container was centered on a rotating carousel in a standard microwave oven (Kenmore model 87425, Sears Roebuck and Co., Chicago IL), irradiated at 200 W (low power) for 120 sec, then immediately removed from the oven. The incubation solution was pipetted off and sections were washed with 0.5mM TRIS pH 7.6 buffer, 250 μl/well, 3 times for 5 min each. The reaction product was intensified by incubation in 0.5% w/v diaminobenzidine (DAB) tetrahydrochloride, 0.00012% v/v hydrogen peroxide in 0.1 M sodium acetate. Completed sections were mounted on subbed slides, dehydrated through ethanol and xylenes, and coverslipped using Eukitt (Calibrated Instruments, Ardsley, NY). Control sections were treated identically except that acetylthiocholine iodide was omitted from the incubation solution. All reagent chemicals were obtained from Sigma Chemical Co. (St. Louis, MO) or Fisher Scientific (Atlanta, GA).

AChE histochemistry precisely and sensitively reflects cholinergic innervation of the dentate gyrus and synaptic reorganization after entorhinal deafferentation, (Deller and Frotscher 1997), including dentate cholinergic remodeling early in AD. We have developed an approach we term *histochemetry* to quantify cholinergic organization in dentate subregions by measuring AChE staining intensity at defined anatomical locations (King et al., 1989). This was used to evaluate potential vector effects on the cholinergic innervation of the dentate. Using the software package ImagePro Plus (Media Cybernetics, Silver Springs, MD), digital 12.5× brightfield microscope images of AChE-labeled sections were collected under equivalent illumination from slides coded to obscure experimental treatment. For each animal the right

and left hippocampus were measured on horizontal sections that most closely matched Plates 98 and 107 of Paxinos & Watson (1986), to sample at approximately 1/3 and 2/3 of the septal-temporal extent. The 8-bit intensity channel was extracted from each 24-bit 640 × 480 pixel hue/saturation/intensity image (Figure 4, E). Lines perpendicular to the granule cell layer (GCL) were manually positioned over the intensity images to define sampling traverses spanning the dentate (Figure 4, B,E). The traverses were placed as close as possible to the midpoint from the vertex to the tip of the buried and exposed blade GCL, at a position where the GCL was relatively uncurved. The traverses extended from the polymorph zone in the dentate hilus to beyond the distal molecular layer, and served as guides for collecting measurements of relative AChE staining intensity. For every image pixel along the line, the gray level values of all the pixels extending 10 pixels perpendicularly on either side of the guide line was averaged. The values provided discrete, smoothed intensity profiles across the dentate reflecting the local density of AChE reaction product (Figure 4, D,F). Characteristic peaks, valleys, and inflections in these profiles were used to identify subfields (infragranular zone (IG), GCL, supragranular zone (SG), associational/commissural terminal field (A/C), middle molecular layer (MML, medial entorhinal terminal field), outer molecular layer (OML, lateral entorhinal terminal field), fissure (F)), and to trim the traverses to begin at the IG/GCL boundary and end at the hippocampal fissure (buried blade) or cisternal space (exposed blade). To normalize for between-sample (side, section, animal) differences in the absolute distance between the GCL and the distal molecular layer border, each trimmed profile was interpolated to a length of 100 points where each point represented 1% of the distance (Figure 4, B). Minor variation in background and signal were probable because it was not possible to perform the AChE histochemistry on all samples simultaneously. To correct for potential differences in background intensity across animals, the difference between the group mean of the 3 maximum GCL gray levels, and the mean for each individual traverse, was added to the gray level for each point along the traverse. The rationale for normalizing to the GCL is that this subfield does not exhibit synaptic reorganization in response to entorhinal deafferentation, and there were no detectable treatment differences in the GCL intensities. Data were analyzed with and without this correction.

Eight traverses representing AChE intensity at 1% intervals across the dentate were generated under treatment-blind conditions for each animal (2 sections, 2 sides each section, 2 blades each side). Repeated-measures (side, section, traverse points) ANOVA was used to test for vector effects at each percent distance along the normalized traverse. Separate analyses were conducted for buried and exposed blades due to intrinsic differences in cholinergic innervation patterns. Dorsal-ventral position (section) effects were tested, as were absolute (pre-normalized) distances across the dentate, and both normalized and raw gray levels.

3. RESULTS

3.1 Histological Results

Injections resulted in reproducible expression in medial and lateral entorhinal cortex (Figure 1). In animals that received GFP control vector, expression 13 weeks post-injection was observed exclusively in neurons located near the injection sites. The GFP filled neurons entirely, revealing projections into the dentate molecular layer and hippocampal stratum lacunosum-moleculare as well as cortical and subcortical retrohippocampal projection domains. Transduced neurons were found throughout approximately the central half of the dorsal-ventral extent of the entorhinal cortex and labeled perforant path axons observed at all septo-temporal levels of the hippocampal formation. Numbers of neuron cell bodies ranged up to several hundred per section for both vectors.

Rats injected with the P301L tau vector also exhibited expression only in neurons. The antibody T14 to human tau revealed tau within dendrites, perikarya, and axons of entorhinal neurons,

including *en passage* synaptic boutons (Figure 2A,B). All P301L tau vector rats exhibited human tau expression in a subpopulation of entorhinal cortex neurons. Antibody AT8 targeted to tau phosphorylated serine residues 202 and 205 labeled a similar but smaller population of neurons as T14 (Figure 2C,D). The NFT antibody recognizing human neurofibrillary tangle tau conformations, however, labeled different objects than the other tau antibodies (Figure 3A,B). Few structures resembling the neuronal perikarya containing neurofibrillary tangles observed in humans were observed. However, numerous irregular objects smaller than neuronal somata were located near the injection sites and in the efferent terminal fields of retrohippocampal neurons. A similar labeling pattern for NFT-positive neurons was revealed by Gallyas silver staining (Figure 3C,D), with a considerable increase in sensitivity compared to NFT immunolabeling. Control-vector or non-transduced tissues were blank for these markers.

Neuronal loss was not obvious by differences in the number of tau- vs. GFP-expressing neurons, FluoroJade B labeling, or qualitative changes in neuronal density in Nissl-stained sections in either entorhinal cortex or hippocampus. Neither astrogliosis (glial fibrillary acidic protein immunolabeling) nor microgliosis (OX-6 immunolabeling) were remarkable for either vector except for the typical mild reaction along the injection needle track (not shown). Previous studies predicted that neuronal loss would be negligible with this vector (AAV2) and survival interval (Klein et al., 2004). Axonal and synaptic pathology, on the other hand, could either precede or accompany death of entorhinal neurons. Thus, we reasoned that examination of dentate gyrus cholinergic synaptic reorganization would be able to detect either mild (DG deafferentation without parent cell death) or severe (outright EC cell loss) neurodegeneration. This synaptic reorganization, as assayed by AChE staining, is exquisitely sensitive to even partial entorhinal deafferentation (Deller and Frotscher, 1997), and occurs in AD (Cotman et al. 1990). Our histochemetric analysis of dentate AChE stain intensity and distribution revealed that no significant synaptic remodeling was detectable in the dentate molecular layer as is typically seen after an electrolytic lesion of the entorhinal area (e.g., Ramirez et al., 2007; and see Figure 4). Because this result is inconsistent with substantial entorhinal cortex neuron loss, stereological cell counts would not be likely to be fruitful and were deferred.

3.2 Behavioral Results

We calculated the rats' daily errors as an average score for 12 one-week blocks. The data were tested to ensure that there were no differences in the grouped rats' daily errors at the beginning of the study. We preceded each of our comparisons with multivariate F-tests to ensure that we did not violate key homogeneity assumptions for our repeated measures analyses. No gross motor abnormalities were observed at any point during behavioral testing.

We conducted a two-way mixed ANOVA to compare GFP Control and Tau groups across those 12 blocks. Tau virus rats made more overall errors ($M = 2.742$) than controls ($M = 1.964$) ($F(1, 18) = 26.945$, MSE = 1.346, $p < .001$, $\eta^2 = .600$). There was a main effect for blocks, wherein errors decreased over time ($F(11,198) = 6.034$, MSE = 0.687, $p < .001$, $\eta^2 = .251$). There was a significant statistical interaction ($F(11,198) = 5.427$, MSE = 0.687, $p < .001$, $\eta^2 = .226$), reflecting significant differences in the trends of errors over time between the two groups. As seen in Figure 5, there is essentially a linear trend showing decreasing errors in the GFP Control group. We tested this assumption with *a priori post hoc* orthogonal contrast analyses, showing a statistically significant linear trend ($F(1,9) = 81.169$, MSE = 0.684, $p < .001$, $\eta^2 = .901$), a robust fit for the linear trend in the decreasing means for the GFP Control group. Similarly, we conducted orthogonal contrast analyses for the Tau group. For the Tau group, the statistically significant trends were curvilinear, for both the quadratic ($F(1,9) = 6.699$, MSE= 0.758, $p< .001$, $\eta^2 = .427$) and cubic ($F(1,9) = 10.128$, MSE = 0.801, $p < .001$,

η^2 = .529) trend orthogonal contrasts across the 12 blocks, showing that the Tau rats' performance returned to baseline levels.

As seen in Figure 5, it appears that errors for rats in the Tau group began a return to baseline drift at the end of week seven. Independent samples *t*-tests were conducted to compare total errors between groups at each week. The groups were statistically different beginning at week seven ($t = -2.280$ (18), $p = .035$), although this result should be interpreted cautiously since it was conducted as a *post hoc* test, and .035 exceeds the value of the Bonferroni correction used for this set of *post hoc* tests (alpha = .004167). From this seven-week point of behavioral testing, the two groups differed significantly at each subsequent week.

4. DISCUSSION

Selective expression of P301L mutated tau centered in the entorhinal region of rats significantly impaired performance on learned spatial alternation. Although acquisition rates for the GFP Control and the Tau groups were similar for the first 6 weeks of postoperative testing, the Tau group was significantly impaired thereafter. Indeed, the Tau group on average had reached as proficient a level of alternation (fewer than 2 errors per session) by the fifth week of testing as the GFP Control group had achieved. In contrast to the GFP Control group, however, the Tau group's performance worsened during the seventh week of testing and remained poorer than the GFP Control group through the twelfth week of testing. Importantly, at the end of behavioral testing the Tau group exhibited extensive evidence of hyperphosphorylated tau and NFTs throughout the entorhinal cortex and retrohippocampal area injected with the rAAV2-tau_{P301L}. It will be important in future studies to characterize the tauopathy when the behavior diverges. Indeed, previous work has shown that tau_{P301L} expression after rAAV2-tau_{P301L} vector injection into rat basal forebrain nuclei or substantia nigra does not reach maximal levels until about 3 to 4 weeks after the injection (Klein et al., 2004; 2008). It is not unlikely, therefore, that expression levels were at a maximum before six weeks, although the tau neuropathology could have continued to accumulate. Even though some signs of neurofibrillary tangles can be found as early as two to three weeks after tau gene transfer (Klein et al., 2004, 2009), the behavioral time-course observed here suggests a slower development of functional tau pathology that may be analogous to progressive dementia.

Transgene proteins located in dentate molecular layer axons indicated that the injections accurately targeted the perforant path. Moreover, the patterns of Gallyas silver stain, and AD conformational tau epitopes in the hippocampus proper and dentate gyrus in rats with entorhinal neurons transduced with the rAAV2-tau_{P301L} vector indicate a vector-induced expression of tau aggregates and neuritic detritus in the synaptic terminal field of the perforant path. These results support the hypothesis that adult-onset tauopathy limited to a subpopulation of entorhinal neurons, including some projecting to hippocampus, is sufficient to impair mnemonic function similar to what is observed in limbic tauopathies. Neither outright neuronal loss nor full degeneration of efferent axons are necessary for the emergence of significant impairment.

Although the precise nature of the entorhinal contribution to spatial memory is under debate (e.g. Eichenbaum and Lipton, 2008), recent evidence (Parron et al., 2006; Ramirez et al., 2007; Sargolini et al., 2006; Steffenach et al., 2005) supports the notion that the EC and adjacent retrohippocampal structures contribute to spatial learning and memory. When tested for retention of a preoperatively learned spatial working memory task, entorhinectomized rats exhibit persistent spatial working memory deficits (Loesche and Steward, 1977; Steward et al., 1977). Additionally, the EC appears to contribute to the acquisition of a spatial alternation task, as bilateral electrolytic entorhinal lesions significantly disrupt spatial learning, which persists for up to 12 weeks of postoperative testing (Ramirez et al., 2007). Some caution should

be exercised in considering these findings as electrolytic lesions injure axons-of-passage, thus some distant structure whose axons course through the site of injury might be contributing to spatial memory function. Neurotoxic lesions, which spare axons-of-passage, have yielded variable outcomes as to severity and duration of mnemonic deficits in rodents, ranging from little to significant impairments (Galani et al., 2002; Jarrard, 1993; Marighetto et al., 1998; Pouzet et al., 1999; Schmadel et al., 2004). Our present findings support the hypothesis that the entorhinal cortex contributes to the performance of a spatial learning and memory task. Despite relatively small and circumscribed EC injections and evidence that entorhinal neurons were selectively transduced by the rAAV2-tau$_{P301L}$, putatively sparing axons-of-passage from injury, rats with the rAAV2-tau$_{P301L}$ injections developed, after 6 weeks of testing, enduring impairments in spatial working memory function that persisted up to 12 weeks after the initiation of behavioral testing. We conclude that a small, but highly-targeted, tau expression in the entorhinal cortex is sufficient to affect memory-related behavior. Even with little evidence for substantial loss of perforant path neurons, vector-induced tauopathy of the perforant path resulted in progressive and persistent impairment of spatial working memory.

Relative entorhinal pathology may in fact explain differences in mnemonic function in relation to global NFT development in transgenic models. In recent years, descriptions of behavioral outcomes of the tau$_{P301L}$ mutation in transgenic mouse models document the complex nature of tau$_{P301L}$ expression and consequent cognitive performance. Following the first demonstration (Lewis et al., 2000) that transgenic mice expressing tau$_{P301L}$ exhibit extensive NFT distribution throughout brain and spinal cord, associated with severe motor impairments, several studies have confirmed that tau$_{P301L}$ expression in transgenic mice also significantly affects cognitive performance. Using a variety of tasks that are sensitive to working memory deficits (e.g. spontaneous alternation and the radial-arm water maze), Arendash et al. (2004) demonstrated that transgenic mice (JNPL3) with the tau$_{P301L}$ mutation had significant negative correlations between the number of tau positive neurons in cortex and hippocampus and the performance on the working memory tasks. As a group, however, the tau$_{P301L}$ mice performed as well as the control animals on these tasks. Thus, it appears that only those animals with the highest tau$_{P301L}$ load evidenced signs of impaired working memory. More recent work suggests that tau$_{P301L}$ mice (TgTau(P301L)23027) at about 12 to 13 months of age with neuronal pretangles and NFTs exhibit impairments on working memory in Morris water maze and eight-arm radial maze, whereas reference memory is intact (Murakami et al., 2006). On the contrary, tau$_{P301L}$ mice at 6 and 11months of age with tau aggregates in a variety of brain regions including the hippocampus and the amygdala exhibit normal working memory on a spontaneous alternation task and on a Morris water maze, but impaired spatial reference memory (Pennanen et al., 2006). In a longitudinal study of transgenic mice (rTg (tau$_{P301L}$) 4510), Ramsden et al. (2005) reported spatial reference memory deficits are not evident at 1.3 months of age, but appear at 4.5 months and continue to worsen through 9.5 months of age. In addition, they observed acquisition deficits appearing as early as 1.3 months that worsened with age, while in our model adult rats acquire the spatial alternation task at similar rates in both GFP- and tau$_{P301L}$ -viral vector groups. In contrast to the variable results amongst different tau overexpression mouse models regarding memory-related behaviors, we have demonstrated that functional effects of tau can be studied over a relatively short time-course of 6–12 weeks when a limited level of tau is restricted to one of the most relevant areas for mnemonic behavior, i.e. the entorhinal area, in fully developed normal rats.

AChE histochemistry reflects cholinergic innervation of the dentate gyrus and synaptic reorganization after entorhinal deafferentation, including dentate cholinergic remodeling early in Alzheimer's disease (reviewed in Ramirez, 2001). The absence of experimental and control group differences in AChE distribution across the dentate molecular layer supports the hypothesis that the behavioral impairment resulting from P301L tau expression in entorhinal cortex is not due to a substantial denervation of hippocampus. Measurable synaptic remodeling

in `early' AD could actually be preceded by detectable, behaviorally relevant hippocampal dysfunction that might provide opportunities for diagnosis and therapy prior to the development of irreversible pathology.

Perhaps owing to differences in tau_{P301L} isoform (i.e., which exons are incorporated), variable expression across forebrain areas and brain development, genetic background, behavioral testing tasks and procedures, as well as age of testing, the impact of the tau_{P301L} mutation on specific mnemonic processes, such as working memory, has been difficult to resolve. The somatic cell gene transfer model explored here provides a well-controlled approach to delivering the P301L tau mutation to particular brain regions implicated in diseases such as AD. The EC and its perforant path output undergo significant pathology early in AD (deToledo-Morrell et al., 2004; Garcia-Sierra et al., 2000; Juottonen et al., 1998; Mitchell et al., 2002; Stoub et al., 2010). The successful targeted delivery of the viral vector into the EC and subsequent expression of NFTs in the entorhinal area and the perforant path supports the use of this approach as a model for exploring the tauopathy associated with dementia. Importantly, significant memory impairments developed in the absence of substantial entorhinal neuron death or even detectable hippocampal deafferentation after the transduction of entorhinal neurons. If the mechanisms responsible for memory dysfunction do not require outright degeneration, then other cellular processes must be causal. Synaptic transmission and plasticity, for example, depend on intact intracellular transport, which is known to be impaired by mutant tau.

The working memory deficit that developed over a period of seven weeks of testing and that persisted for up to five weeks of testing after its onset lends credence to the use of this approach to model progressively dementing neurodegenerative tauopathies such as AD (Belleville et al., 2008; Germano and Kinsella, 2005). Precise control over the localization and timing of tau pathology to brain regions that contribute to learning and memory, and which are centrally involved in AD, makes the somatic transgenic approach advantageous for exploring disease mechanisms and therapeutic interventions. Indeed, the induction of asymptotic P301L expression and the subsequent development of tauopathy and mnemonic impairment indicate that this is a useful, temporally defined, efficient model for studying causal relationships among tau, synaptic, and mnemonic functions.

Acknowledgments

Supported by grants from the National Institutes of Health (MH060608) and the Howard Hughes Medical Institute (52005120) to JJR, the National Institutes of Health (NIA P10485) and U.S. Department of Veterans Affairs to MAK, and the National Institutes of Health (NS048450) to RLK.

REFERENCES

Arendash GW, Lewis J, Leighty RE, McGowan E, Cracchiolo JR, Hutton M, Garcia MF. Multi-metric behavioral comparison of APPsw and P301L models for Alzheimer's disease: linkage of poorer cognitive performance to tau pathology in forebrain. Brain Res 2004;1012:29–41. [PubMed: 15158158]

Belleville S, Sylvain-Roy S, de Boysson C, Menard MC. Characterizing the memory changes in persons with mild cognitive impairment. Prog. Brain Res 2008;169:365–375. [PubMed: 18394487]

Braak H, Braak E. Neuropathological stageing of Alzheimer-related changes. Acta Neuropathol 1991;82:239–259. [PubMed: 1759558]

Brunden KR, Trojanowski JQ, Lee VMY. Evidence that non-fibrillar tau causes pathology linked to neurodegeneration and behavioral impairments. J Alzheimers Dis 2008;14:393–399. [PubMed: 18688089]

Buée L, Bussiere T, Buée-Scherrer V, Delacourte A, Hof PR. Tau protein isoforms, phosphorylation and role in neurodegenerative disorders. Brain Res. Brain Res. Rev 2000;33:95–130. [PubMed: 10967355]

Carter J, Lippa CF. Beta-amyloid, neuronal death and Alzheimer's disease. Curr. Mol. Med 2001;1:733–737. [PubMed: 11899259]

Cotman CW, Geddes JW, Kahle JS. Axon sprouting in the rodent and Alzheimer's disease brain: a reactivation of developmental mechanisms? Prog. Brain Res 1990;83:427–34. [PubMed: 2203106]

Deller T, Frotscher M. Lesion-induced plasticity of central neurons sprouting of single fibres in the rat hippocampus after unilateral entorhinal cortex lesion. Prog. Neurobiol 1997;53:687–727. [PubMed: 9447617]

deToledo-Morrell L, Stoub TR, Bulgakova M, Wilson RS, Bennett DA, Leurgans S, Wuu J, Turner DA. MRI-derived entorhinal volume is a good predictor of conversion from MCI to AD. Neurobiol. Aging 2004;25:1197–1203. [PubMed: 15312965]

Eichenbaum H, Lipton PA. Towards a functional organization of the medial temporal lobe memory system: role of the parahippocampal and medial entorhinal cortical areas. Hippocampus 2008;18:1314–1324. [PubMed: 19021265]

Eriksen JL, Janus CG. Plaques, tangles, and memory loss in mouse models of neurodegeneration. Behav. Genet 2007;37:79–100. [PubMed: 17072762]

Galani R, Obis S, Coutureau E, Jarrard L, Cassel JC. A comparison of the effects of fimbria-fornix, hippocampal, or entorhinal cortex lesions on spatial reference and working memory in rats: short versus long postsurgical recovery period. Neurobiol. Learn. Mem 2002;77:1–16. [PubMed: 11749082]

Gallyas F. Silver staining of Alzheimer's neurofibrillary changes by means of physical development. Acta Morphol. Acad. Sci. Hung 1971;19:1–8. [PubMed: 4107507]

Garcia-Sierra F, Hauw JJ, Duyckaerts C, Wischik CM, Luna-Munoz J, Mena R. The extent of neurofibrillary pathology in perforant pathway neurons is the key determinant of dementia in the very old. Acta neuropathol 2000;100:29–35. [PubMed: 10912917]

Gellerman LW. Chance orders of alternative stimuli in visual discrimination experiments. J. Genetic Psychol 1933;42:206–208.

Germano C, Kinsella GJ. Working memory and learning in early Alzheimer's disease. Neuropsychol. Rev 2005;15:1–10. [PubMed: 15929495]

Giannakopoulos P, Herrmann FR, Bussiere T, Bouras C, Kovari E, Perl DP, Morrison JH, Gold G, Hof PR. Tangle and neuron numbers, but not amyloid load, predict cognitive status in Alzheimer's disease. Neurology 2003;60:1495–1500. [PubMed: 12743238]

Hyman BT, Van Hoesen GW, Damasio AR, Barnes CL. Alzheimer's disease: Cell-specific pathology isolates the hippocampal formation. Science 1984;225:1168–1170. [PubMed: 6474172]

Hymn BT, Van Hoesen GW, Kromer LJ, Damasio AR. Perforant pathway changes and the memory impairment of Alzheimer's disease. Ann. Neurol 1986;20:472–481. [PubMed: 3789663]

Ikeda K, Haga C, Oyanagi S, Iritani S, Kosaka K. Ultrastructural and immunohistochemical study of degenerate neurite-bearing ghost tangles. J Neurol 1992;239:191–194. [PubMed: 1597685]

Jarrard LE. On the role of the hippocampus in learning and memory in the rat. Behav. Neural Biol 1993;60:9–26. [PubMed: 8216164]

Juottonen K, Laakso MP, Insausti R, Lehtovirta M, Pitkanen A, Partanen K, Soininen H. Volumes of the entorhinal and perirhinal cortices in Alzheimer's disease. Neurobiol. Aging 1998;19:15–22. [PubMed: 9562498]

Karnovsky MJ, Roots L. A “direct-coloring” thiocholine method for cholinesterases. J. Histochem. Cytochem 1964;12:219–221. [PubMed: 14187330]

King MA, Walker DW, Hunter BE, Reep RL. Acetylcholinesterase stain intensity patterns in the rat dentate gyrus: A quantitative description based on digital image analysis. Neurosci 1989;33:203–231.

Klein RL, Dayton RD, Leidenheimer NJ, Jansen K, Golde TE, Zweig RM. Efficient neuronal gene transfer with AAV8 leads to neurotoxic levels of tau or green fluorescent proteins. Mol. Ther 2006;13:517–527. [PubMed: 16325474]

Klein RL, Dayton RD, Diaczynsky CG, Wang DB. Pronounced microgliosis and neurodegeneration in aged rats after tau gene transfer. Neurobiol. Aging. 2009 in press.

Klein RL, Dayton RD, Tatom JB, Diaczynsky CG, Salvatore MF. Tau expression levels from various adeno-associated virus vector serotypes produce graded neurodegenerative disease states. Eur. J. Neurosci 2008;27:1615–1625. [PubMed: 18380664]

Klein RL, Lin WL, Dickson DW, Lewis J, Hutton M, Duff K, Meyer EM, King MA. Rapid neurofibrillary tangle formation after localized gene transfer of mutated tau. Am. J. Pathol 2004;164:347–353. [PubMed: 14695347]

Lewis J, McGowan E, Rockwood J, Melrose H, Nacharaju P, Van Slegtenhorst M, Gwinn-Hardy K, Murphy MP, Baker M, Yu X, Duff K, Hardy J, Corral A, Lin WL, Yen SH, Dickson DW, Davies P, Hutton M. Neurofibrillary tangles, amyotrophy and progressive motor disturbance in mice expressing mutant (P301L) tau protein. Nat. Genet 2000;25:402–405. [PubMed: 10932182]

Loesche J, Steward O. Behavioral correlates of denervation and reinnervation of the hippocampal formation of the rat: recovery of alternation performance following unilateral entorhinal cortex lesions. Brain Res. Bull 1977;2:31–39. [PubMed: 861769]

Marighetto A, Yee BK, Rawlins JN. The effects of cytotoxic entorhinal lesions and electrolytic medial septal lesions on the acquisition and retention of a spatial working memory task. Exp. Brain Res 1998;119:517–528. [PubMed: 9588787]

Mitchell TW, Mufson EJ, Schneider JA, Cochran EJ, Nissanov J, Han LY, Bienias JL, Lee VM, Trojanowski JQ, Bennett DA, Arnold SE. Parahippocampal tau pathology in healthy aging, mild cognitive impairment, and early Alzheimer's disease. Ann. Neurol 2002;51:182–189. [PubMed: 11835374]

Murakami T, Paitel E, Kawarabayashi T, Ikeda M, Chishti MA, Janus C, Matsubara E, Sasaki A, Kawarai T, Phinney AL, Harigaya Y, Horne P, Egashira N, Mishima K, Hanna A, Yang J, Iwasaki K, Takahashi M, Fujiwara M, Ishiguro K, Bergeron C, Carlson GA, Abe K, Westaway D, St. George-Hyslop P, Shoji M. Cortical neuronal and glial pathology in TgTauP301L transgenic mice: neuronal degeneration, memory disturbance, and phenotypic variation. Am. J. Pathol 2006;169:1365–1375. [PubMed: 17003492]

Parron C, Poucet B, Save E. Cooperation between the hippocampus and the entorhinal cortex in spatial memory: a disconnection study. Behav. Brain Res 2006;170:99–109. [PubMed: 16540184]

Paxinos, G.; Watson, C. The rat brain in stereotaxic coordinates. Academic Press; New York: 1986.

Pennanen L, Wolfer DP, Nitsch RM, Gotz J. Impaired spatial reference memory and increased exploratory behavior in P301L tau transgenic mice. Genes Brain Behav 2006;5:369–379. [PubMed: 16879631]

Pouzet B, Welzl H, Gubler MK, Broersen L, Veenman CL, Feldon J, Rawlins JN, Yee BK. The effects of NMDA-induced retrohippocampal lesions on performance of four spatial memory tasks known to be sensitive to hippocampal damage in the rat. Eur. J. Neurosc 1999;11:123–140.

Ramirez JJ. The role of axonal sprouting in functional reorganization after CNS injury: lessons from the hippocampal formation. Restor. Neurol. Neurosci 2001;19:237–262. [PubMed: 12082224]

Ramirez JJ, Campbell D, Poulton W, Barton C, Swails J, Geghman K, Courchesne SL, Wentworth S. Bilateral entorhinal cortex lesions impair acquisition of delayed spatial alternation in rats. Neurobiol. Learn. Mem 2007;87:264–268. [PubMed: 17049284]

Ramirez JJ, Stein DG. Sparing and recovery of spatial alternation performance after entorhinal cortex lesions in rats. Behav. Brain Res 1984;13:53–61. [PubMed: 6477719]

Ramsden M, Kotilinek L, Forster C, Paulson J, McGowan E, SantaCruz K, Guimaraes A, Yue M, Lewis J, Carlson G, Hutton M, Ashe KH. Age-dependent neurofibrillary tangle formation, neuron loss, and memory impairment in a mouse model of human tauopathy (P301L). J. Neurosci 2005;25:10637–10647. [PubMed: 16291936]

Santacruz K, Lewis J, Spires T, Paulson J, Kotilinek L, Ingelsson M, Guimaraes A, DeTure M, Ramsden M, McGowan E, Forster C, Yue M, Orne J, Janus C, Mariash A, Kuskowski M, Hyman B, Hutton M, Ashe KH. Tau suppression in a neurodegenerative mouse model improves memory function. Science 2005;309:476–481. [PubMed: 16020737]

Sargolini F, Fyhn M, Hafting T, McNaughton BL, Witter MP, Moser MB, Moser EI. Conjunctive representation of position, direction, and velocity in entorhinal cortex. Science 2006;312:758–762. [PubMed: 16675704]

Schmadel S, Schwabe K, Koch M. Effects of neonatal excitotoxic lesions of the entorhinal cortex on cognitive functions in the adult rat. Neuroscience 2004;128:365–374. [PubMed: 15350648]

Sinha S, Lieberburg I. Cellular mechanisms of beta-amyloid production and secretion. Proc. Natl. Acad. Sci 1999;96:11049–11053. [PubMed: 10500121]

Spires TL, Orne JD, SantaCruz K, Pitstick R, Carlson GA, Ashe KH, Hyman BT. Region-specific dissociation of neuronal loss and neurofibrillary pathology in a mouse model of tauopathy. Am. J. Pathol 2006;168:1598–1607. [PubMed: 16651626]

Steffenach HA, Witter M, Moser MB, Moser EI. Spatial memory in the rat requires the dorsolateral band of the entorhinal cortex. Neuron 2005;45:301–313. [PubMed: 15664181]

Steward O, Loesche J, Horton WC. Behavioral correlates of denervation and reinnervation of the hippocampal formation of the rat: open field activity and cue utilization following bilateral entorhinal cortex lesions. Brain Res. Bull 1977;2:41–48. [PubMed: 861770]

Stoub TR, Rogalski EJ, Leurgans S, Bennett DA, deToledo-Morrell L. Rate of entorhinal and hippocampal atrophy in incipient and mild AD: Relation to memory function. Neurobiol. Aging 2010;31:1089–1098. [PubMed: 18809228]

Thal DR, Holzer M, Rub U, Waldmann G, Gunzel S, Zedlick D, Schober R. Alzheimer-related tau-pathology in the perforant path target zone and in the hippocampal stratum oriens and radiatum correlates with onset and degree of dementia. Exp. Neurol 2000;163:98–110. [PubMed: 10785448]

Tolnay M, Probst A. Frontotemporal lobar degeneration--tau as a pied piper? Neurogenetics 2002;4:63–75. [PubMed: 12481984]

Tolnay M, Probst A. REVIEW: tau protein pathology in Alzheimer's disease and related disorders. Neuropathol. Appl. Neurobiol 1999;25:171–187. [PubMed: 10417659]

Wasling P, Daborg J, Riebe I, Andersson M, Portelius E, Blennow K, Hanse E, Zetterberg H. Synaptic retrogenesis and amyloid-beta in Alzheimer's disease. J. Alzheimers Dis 2009;16:1–14. [PubMed: 19158416]

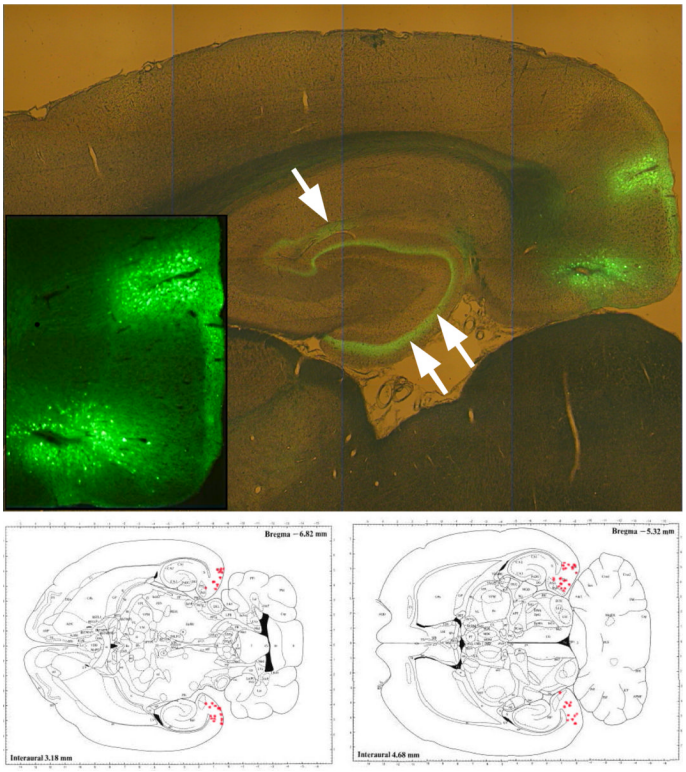

Figure 1.
Control rAAV (constructed to drive the expression of GFP) injection led to a robust expression in layers II and III of the entorhinal cortex (inset), with efferents projecting to the dentate gyrus molecular layer (double arrow) and stratum lacunosum-moleculare of regio superior (single arrow). Panels below, reconstructions of transgene expression in entorhinal cortex [modified from Paxinos and Watson, 1986]. Each dot in the retrohippocampal area indicates the estimated center of transgene expression for each rat, at two positions along the dorsal-ventral axis.

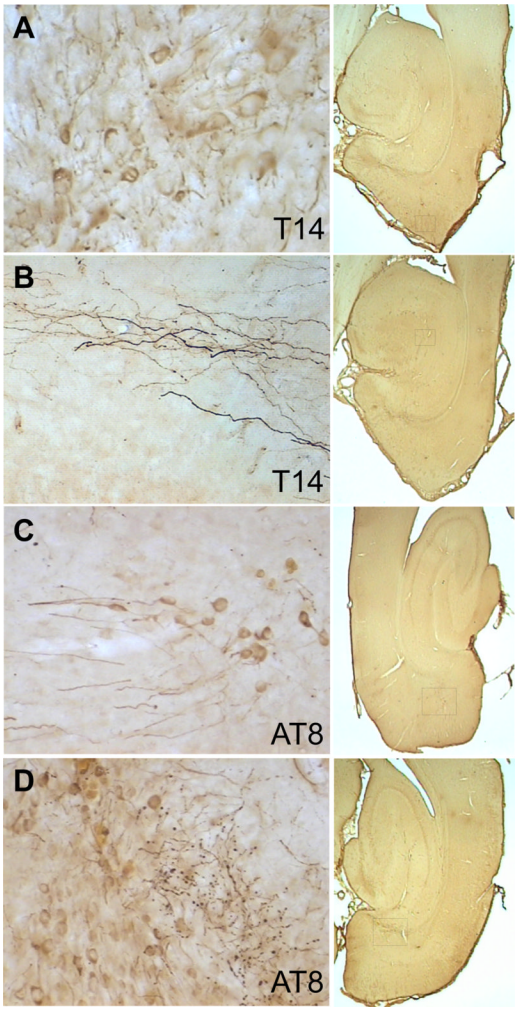

Figure 2.

Human tau immunoreactivity was distributed throughout all neuronal cytoplasmic compartments including perikarya, dendrites (panel A, entorhinal cortex), and axons (panel B, presumptive perforant path projections in dentate gyrus). Hyperphosphorylated tau was similarly localized in somata, dendrites (panel C, entorhinal cortex), axons and synaptic boutons (panel D, presubiculum). Controls were blank for human tau immunoreactivity. Boxes in the 1× images at right show the approximate location of each higher-magnification frame.

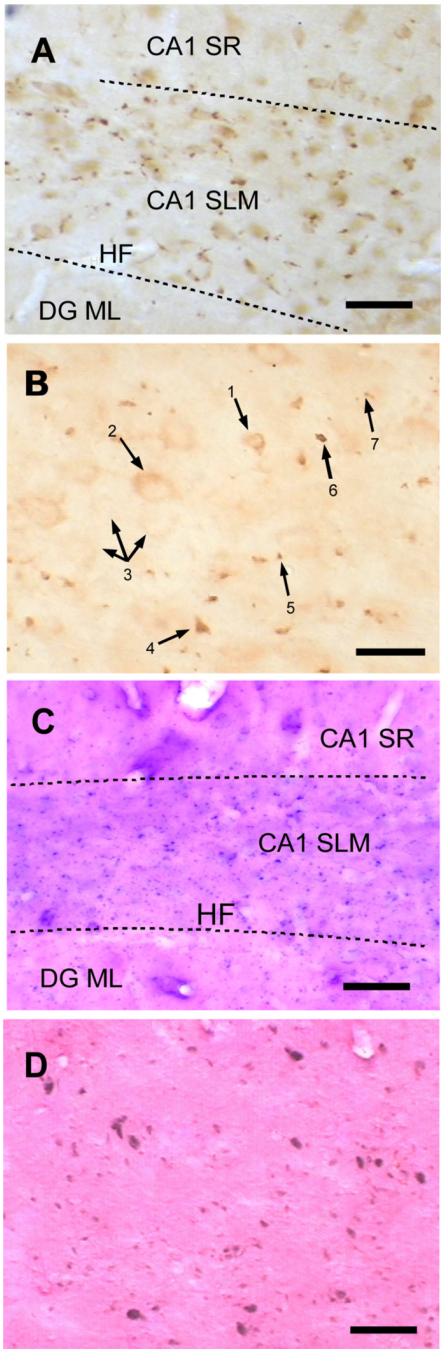

Figure 3.

A. Immunolabeling for neurofibrillary tangle antigen in CA1 stratum lacunosum moleculare entorhinal terminal field. The absence of labeling in stratum radiatum is indicative of control sections processed without primary antibody. B. Immunolabeling for neurofibrillary tangle tau in entorhinal cortex: Small (1) and large (2) neurons exhibited perikaryal NFT tau, in close proximity to other neurons (3) that showed no labeling. A few strongly immunoreactive objects smaller than neurons resembled ghost tangles (4; cf. Ikeda, Haga, Oyanagi, Iritani, and Kosaka, 1992). Other small densely labeled objects may be glia (6) but some are too small and are more likely to be degenerated neuronal processes (5, 7). C. Argentophilic Gallyas staining in similar

field to A. D. Gallyas staining in entorhinal cortex shows several NFT along with smaller degeneration detritus. Scale bars = 50 μm in A, C, D and 25 μm in B.

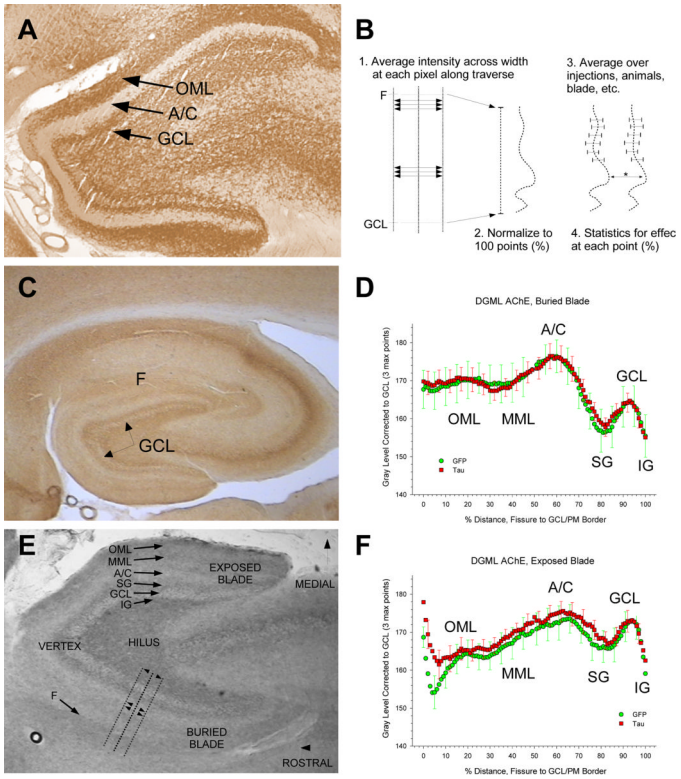

Figure 4.

Quantitative assessment of reactive cholinergic synaptic reorganization in the dentate gyrus molecular layer found no evidence for significant entorhinal deafferentation. A, Reference section from an entorhinal cortex lesion study rat illustrates the 4 cardinal histological phenomena associated with synaptic reorganization: intensification of AChE (1) and narrowing of the dentate outer molecular layer (OML)(2), expansion (3) of the associational/commissural (A/C) terminal field plus clearance of A/C AChE (4). B: Schematic of the AChE histochemetry. Normalized stain intensity values were generated for each 1% distance across the dentate by successively averaging 20 pixel-wide traverses orthogonal to the granule cell layer. C, E: 2 representative rats that received entorhinal rAAV2-tau$_{P301L}$ are qualitatively indistinguishable from control rats. E demonstrates the 8-bit intensity channel on which measurements were made, and anatomical nomenclature used in describing the methods and results. None of the four cardinal effects were evident. D, F: Overlays of group mean (±S.E.M.) traverses from rAAV2-tau$_{P301L}$ (N=6 rats) and rAAV2-GFP (N=6 rats) brains show identical AChE intensity and spatial distribution patterns in the buried (C) and exposed (F) blade.

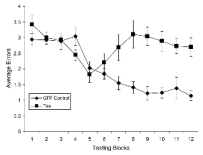

Figure 5.

Rats that sustained bilateral injections of rAAV2-tau$_{P301L}$ were significantly impaired in the retention of reinforced spatial alternation performance, although not in the acquisition of the task. The Tau group committed significantly more errors (*p's* ≤ .035) than the GFP-injected beginning about the seventh week of testing through the end of the study in the twelfth week. (Error bars = ±S.E.M.).